A Blind Adaptation Algorithm for Decision Feedback Equalization for Dual-Mode CAP-QAM Reception

Roland Zukunft, Sven Haar, and Thomas Magesacher

Institute for Integrated Circuits - BRIDGELAB
Munich University of Technology
Arcisstraße 21, D-80290 Munich, Germany

Abstract– **This paper introduces an algorithm for blind adaptation of decision feedback equalizers (DFE), which is applied for equalization in the passband domain. The transmission scheme, which is assumed to be unknown at the receiver side, can either be carrierless amplitude/phase (CAP) modulation or quadrature amplitude modulation (QAM). As the input signal of the passband equalizer is real-valued, the tap weights of the complex-valued feedback filter cannot be identified by a standard whitening approach. We propose therefore an algorithm, which determines a starting coefficient set by means of an infinite impulse response (IIR) equalizer updated by constant modulus algorithm (CMA). For stability reasons, the equalizer's feedback filter is implemented in lattice structure during acquisition. In case of QAM transmission, its tap weights have to be rotated before switching to the DFE. The feedback filter is then fed by the soft decision in order to minimize the probability of wrong solutions.**

I. INTRODUCTION

Carrierless amplitude/phase (CAP) modulation and quadrature amplitude modulation (QAM) are two bandwidth-efficient transmission schemes. A technique to blindly adapt a linear passband equalizer for the both closely related line codes was proposed in [1]. This technique can furthermore determine whether CAP or QAM is employed for transmission. It can e.g. be applied successfully to very high speed digital subscriber line (VDSL) systems, for which it has been proposed [2] that both line codes can be used, while blind adaptation is assumed.

It is however commonly accepted that a decision feedback equalizer (DFE) offers better performance than its linear counterpart for most scenarios, especially for those limited by intersymbol interference (ISI). Our goal is therefore to develop a blind adaptation technique for DFEs employed in the passband domain. As the input of the equalizer is a real-valued passband signal, the technique introduced in [3], which approximates the tap weights of the feedback filter by whitening the equalizer's input signal, can not be directly applied to our scenario. The analytic signal of the input would have to be generated by a Hilbert transformer in this case, resulting in increased hardware complexity. We present therefore a technique, to determine an initial set of DFE parameters by minimizing the constant modulus (CM) cost function [4] by an infinite impulse response (IIR) filter. As direct-form IIR filters may become instable during coefficient adaptation, we present a lattice filter implementation of the CM algorithm (CMA), which allows easy stability monitoring. A different IIR-CMA implementation in normalized lattice structure has been proposed in [5] for PAM transmission. As our filter has to be complex-valued, we apply a technique implementing the lattice filter in the two-multiplier form, which is well suited in this case.

If the CMA-updated equalizer succeeds to open the eye during acquisition mode, the applied transmission scheme is determined at the receiver side and the algorithm is switched to tracking mode, using decision directed (DD) adaptation. Stability monitoring is then not needed anymore, so that the feedback filter can be implemented in the more hardware-efficient direct form. The tap weights are therefore transformed with a simple recursive algorithm. This calculation can be performed offline, if we assume the channel to be only slowly time-varying. If the transmission scheme turns out to be QAM, the parameters of the feedback filter have furthermore to be rotated.

II. SYSTEM MODEL

Consider first the output signal of a conventional baseband QAM transmitter given by

$$s(t) = \mathrm{Re}\left\{\left(\sum_{n=-\infty}^{\infty} A_n g(t-nT)\right)e^{j\omega_c t}\right\}, \qquad (1)$$

where $A_n = a_n + jb_n$ denotes the transmit symbol, ω_c is the carrier angular frequency, T is the symbol period, and $g(t)$ is the lowpass shaping filter. Fig. 1 shows the system model of a QAM transmission system with pulse-shaping filters $p(t) = g(t)\cos\omega_c t$ and $\tilde{p}(t) = g(t)\sin\omega_c t$ implemented as passband shaping filters. For equivalence to the baseband transmitter, the symbols A_n' are rotated versions of A_n:

$$A_n' = A_n e^{j\omega_C nT}. \qquad (2)$$

This rotation can be considered as a recoding of the transmit-symbols which has to be reversed at the receiver side. If the two rotators are removed, the CAP modulation scheme is obtained.

The observation at the receiver input is given by L subchannels

$$\boldsymbol{r}(n) = \left[r(n)^{(1)}\ r(n)^{(2)}\ \dots\ r(n)^{(L)}\right]^{\mathrm{T}}, \qquad (3)$$

modeling the temporal diversity caused by the oversampling, where each subchannel is given by

$$r^{(l)}(n) = \mathrm{Re}\{A_n' H_l(q^{-1})\} + v^{(l)}(n), \qquad (4)$$

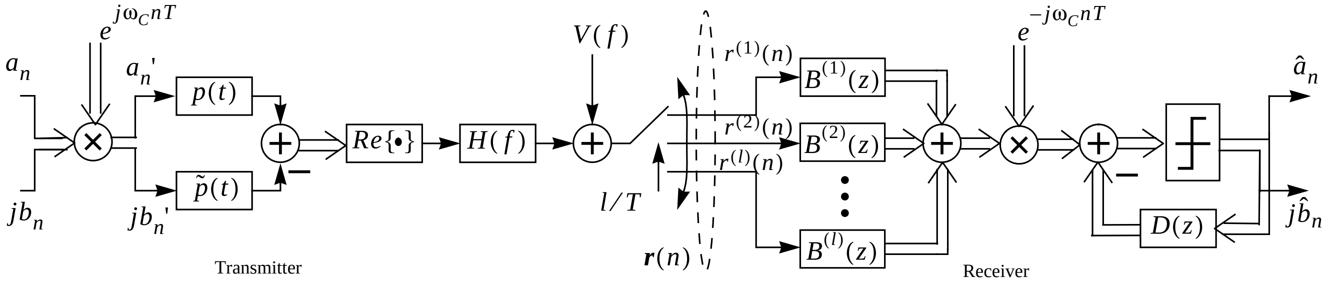

Fig. 1. Passband model of QAM transmission.

and q^{-1} denotes the unit-shift operator.

The discrete channel $\boldsymbol{H}(z)$ is composed of L finite impulse response (FIR) filters of length N_H combining the impulse responses of the pulse-shaping filters and the transmission channel. In the frequency domain it is given by

$$H_l(z) = \sum_{i=0}^{N_H} h_i^{(l)} z^{-i} . \qquad (5)$$

The noise is composed of L independent Gaussian processes $v^{(l)}(n)$ with variance σ_n^2.

The DFE shown in Fig. 1 consists of the fractionally-spaced (FS) feedforward filter $\boldsymbol{B}(z) = [B^1(z)\ B^2(z)\ \dots\ B^l(z)]$ operating in the passband domain with real-valued input samples $\{\boldsymbol{r}\}$, followed by the feedback filter $D(z)$ whose input are sliced symbols $\hat{A}_n(n) = \hat{a}_n + j\hat{b}_n$. The rotator required in the case of QAM transmission is located at the output of the forward equalizer, i.e. the output of the DFE is substracted from the backrotated symbols.

III. Proposed Algorithm

A. Equalizer Structure

The structure of the IIR equalizer in cascade lattice form [6] is shown in Fig. 2. It consists of a feedforward filter with $L \cdot N$-element coefficient row-vector

$$\boldsymbol{b}(n) = \left[\boldsymbol{b}_0(n)\ \boldsymbol{b}_1(n)\ \dots\ \boldsymbol{b}_{N-1}(n)\right], \qquad (6)$$

where N is the number of taps per subchannel and

$$\boldsymbol{b}_k(n) = \left[b_k^{(1)}(n)\ b_k^{(2)}(n)\ \dots\ b_k^{(l)}(n)\right], \qquad (7)$$

followed by an M-tap feedback filter with coefficients represented by row-vector

$$\boldsymbol{k}(n) = \left[k_0(n)\ k_1(n)\ \dots\ k_{M-1}(n)\right]. \qquad (8)$$

The equalizer output $y(n)$ is given by

$$y(n) = \boldsymbol{b}(n-1)\boldsymbol{R}(n) - \boldsymbol{k}(n-1)\boldsymbol{X}(n), \qquad (9)$$

where $\boldsymbol{R}(n) = [\boldsymbol{r}^T(n)\ \boldsymbol{r}^T(n-1)\ \dots\ \boldsymbol{r}^T(n-N+1)]^T$ collects the N preceding L–element vectors of input samples and the state vector of the lattice filter is given by $\boldsymbol{X}(n) = [x_0(n)\ x_1(n)\ \dots\ x_{M-1}(n)]^T$. It follows from Fig. 2, that $\boldsymbol{X}(n+1)$ is given by

$$\boldsymbol{X}(n+1) = \boldsymbol{Q}(n)\boldsymbol{X}(n) + \boldsymbol{P}(n)u(n), \qquad (10)$$

where $\boldsymbol{P}(n) = [1\ k_0(n)\ k_1(n)\ \dots\ k_{M-2}(n)]^T$, $u(n)$ is the output of the forward filter and the $M \times M$ matrix $Q(n)$ is given by

$$\boldsymbol{Q} = \begin{bmatrix} -k_0 & -k_1 & -k_2 & \cdots & -k_{M-1} \\ (1-k_0^2) & -k_0k_1 & -k_0k_2 & \cdots & -k_0k_{M-1} \\ 0 & (1-k_1^2) & -k_1k_2 & \cdots & -k_1k_{M-1} \\ \vdots & \ddots & \ddots & & \vdots \\ 0 & \dots 0(0) & \cdots & (1-k_{M-1}^2) & -k_{M-2}k_{M-1} \end{bmatrix} . \qquad (11)$$

Stability monitoring of the lattice filter is very simple, as one solely has to ensure that the absolute values of the feedback filter tap weights stay below one [6]. Strictly speaking, this condition guarantees bounded input bounded output (BIBO) stability only in steady state. However, extensive simulations indicate that this condition works also well for adapted filters of the considered structure [7].

B. IIR-CMA for the considered equalizer structure

The equalizer parameters can be collected in the vector

$$\boldsymbol{w}_l(n) = \left[\boldsymbol{b}(n)\ \boldsymbol{k}(n)\right], \qquad (12)$$

where the subscript l indicates the lattice structure. They are updated in order to minimize the CM cost function

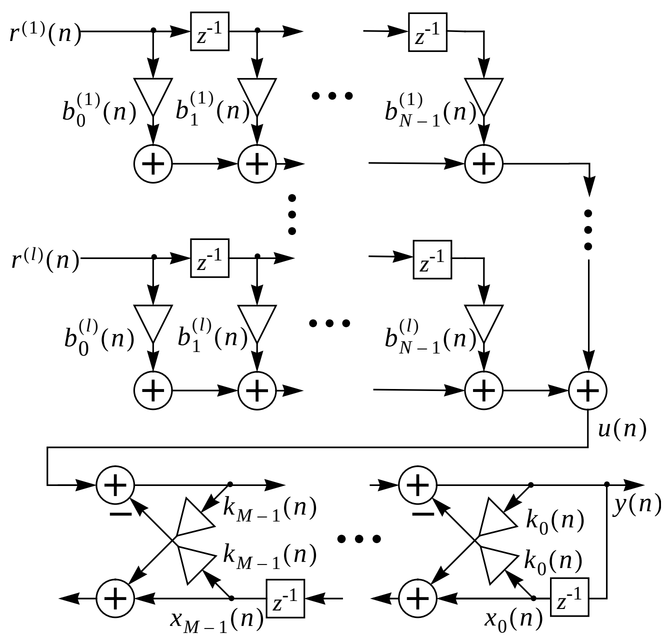

Fig. 2. IIR equalizer structure.

$$J(\boldsymbol{w}_l) = \mathrm{E}\{(|y|^2 - \gamma)^2\}, \qquad (13)$$

where $\gamma = \mathrm{E}\{|y(n)|^4\}/\mathrm{E}\{|y(n)|^2\}$ and $\mathrm{E}\{\cdot\}$ means expectation. The corresponding CMA can be derived by omitting the expectation in (13), calculating the gradient with respect to $\boldsymbol{w}_l(n)$ and correcting the equalizer parameters slightly in the opposite direction, where μ is a small positive step-size:

$$\boldsymbol{w}_l(n+1) = \boldsymbol{w}_l(n) - \frac{1}{2}\mu \frac{\partial J}{\partial \boldsymbol{w}_l}\bigg|_{\boldsymbol{w}_l(n)} =$$

$$\boldsymbol{w}_l(n) - \mu(|y(n)|^2 - \gamma)\frac{\partial}{\partial \boldsymbol{w}_l}|y(n)|^2. \qquad (14)$$

Following [6], the gradient on the right hand side of (14) can be determined as

$$\frac{\partial}{\partial \boldsymbol{w}_l}|y(n)|^2 = \frac{\partial \boldsymbol{w}_d}{\partial \boldsymbol{w}_l^{\mathrm{T}}}\frac{\partial}{\partial \boldsymbol{w}_d}|y(n)|^2, \qquad (15)$$

where $\boldsymbol{w}_d = [\boldsymbol{b}\ \boldsymbol{a}]$ is the corresponding direct form filter with feedback filter taps $\boldsymbol{a} = [a_1\ a_2\ ...\ a_M]$. The relation between $\boldsymbol{k}$ and $\boldsymbol{a}$ is given by the $M \times M$ transformation matrix $\boldsymbol{T}_M$ [6]

$$\boldsymbol{a}(n) = \boldsymbol{k}(n)\boldsymbol{T}_M(n-1), \qquad (16)$$

where $\boldsymbol{T}$ is recursively defined as $\boldsymbol{T}_1 = 1$ and

$$\boldsymbol{T}_m = \begin{bmatrix} \boldsymbol{T}_{m-1} & \begin{matrix} 0 \\ \vdots \\ 0 \end{matrix} \\ k_{m-1}\ [k_{m-1}k_1\ \dots\ k_{m-1}k_{m-2}\ \ 1] \cdot \boldsymbol{T}_{m-1} & \end{bmatrix}. \qquad (17)$$

Making use of the standard slow convergence property, i.e. assuming $\boldsymbol{w}_d(n) = \boldsymbol{w}_d(n-1)$, the gradient signals of the direct form filter are given by [7],[8]

$$\frac{\partial}{\partial b_i^{(l)}}|y(n)|^2 = 2y(n)\zeta_i^{(l)}(n)^* \qquad (18)$$

$$\zeta_i^{(l)}(n) = r^{(l)}(n-i) - \sum_{k=1}^{M} a_k(n-1)\zeta_i^{(l)}(n-k) \qquad (19)$$

$$\frac{\partial}{\partial a_i}|y(n)|^2 = -2y(n)\psi_i(n)^* \qquad (20)$$

$$\psi_i(n) = y(n-i) - \sum_{k=1}^{M} a_k(n-1)\psi_i(n-k). \qquad (21)$$

With $\frac{\partial \boldsymbol{a}}{\partial \boldsymbol{k}^T} = \boldsymbol{T}(n-1) + \boldsymbol{k}(n)\frac{\partial}{\partial \boldsymbol{k}^{\mathrm{T}}}\boldsymbol{T}(n-1)$ [6], we can write

$$\frac{\partial}{\partial \boldsymbol{k}^{\mathrm{T}}}|y(n)|^2 = -2y(n)\left(\boldsymbol{X}_A(n)^* + \boldsymbol{k}(n)\frac{d}{d\boldsymbol{k}^{\mathrm{T}}}\boldsymbol{X}_A(n)^*\right), \qquad (22)$$

where $\boldsymbol{X}_A(n) = \boldsymbol{T}(n-1)\boldsymbol{Y}_A(n)$ is the state vector of the lattice filter with coefficient vector $\boldsymbol{k}(n-1)$ and input $y(n)$. Using once more the slow convergence property [7], $\boldsymbol{Y}_A(n)$ can be written as

$$\boldsymbol{Y}_A(n) = \left[\psi(n)\ \psi(n-1)\ \dots\ \psi(n-(M+1))\right]^{\mathrm{T}}. \qquad (23)$$

In an analog way $\boldsymbol{R}_A(n)$ is formed by the N preceding outputs of L lattice filters with input $r^{(l)}(n)$, and state $\boldsymbol{X}_R^{(l)}(n)$ as

$$\boldsymbol{R}_A(n) = \left[\zeta(n)^{\mathrm{T}}\ \zeta(n-1)^{\mathrm{T}}\ \dots\ \zeta(n-(N+1))^{\mathrm{T}}\right]^{\mathrm{T}}. \qquad (24)$$

An offline version of the model shown in Fig. 2, with $\boldsymbol{X}(n)$ generated by fixed parameters, yields to a simplified version of (22) with vanishing second term [6],[7]. Substitution into the online version results in the simplified algorithm

$$\begin{bmatrix} \boldsymbol{b}(n) \\ \boldsymbol{k}(n) \end{bmatrix} = \begin{bmatrix} \boldsymbol{b}(n-1) \\ \boldsymbol{k}(n-1) \end{bmatrix} - \mu(|y(n)|^2 - \gamma)y(n)\begin{bmatrix} \boldsymbol{R}_A(n)^{\mathrm{H}} \\ -\boldsymbol{X}_A(n)^{\mathrm{H}} \end{bmatrix}, \qquad (25)$$

$$\boldsymbol{X}_R^{(l)}(n) = \boldsymbol{Q}(n-1)\boldsymbol{X}_R^{(l)}(n-1) + \boldsymbol{P}(n-1)r^{(l)}(n), \qquad (26)$$

$$\zeta^{(l)}(n) = -\boldsymbol{k}(n-1)\boldsymbol{X}_R^{(l)}(n-1) + r^{(l)}(n), \qquad (27)$$

$$\boldsymbol{X}_A(n) = \boldsymbol{Q}(n-1)\boldsymbol{X}_A(n-1) + \boldsymbol{P}(n-1)y(n). \qquad (28)$$

It can be seen in (13), that the CMA-adapted equalizer is blind to a rotation of the constellation. To obtain the correct orientation, the actual phase-error θ is estimated and the equalizer output is multiplied by $e^{-j\theta}$. The required device, e.g. the second order phase-tracking loop as suggested in [3], is located behind the rotator shown in Fig. 1. Alternatively, the dual-mode multimodulus algorithm could be employed for equalizer updating as proposed in [1] for linear equalizers.

C. Simplified Equalizer Algorithms applying Feintuch Updates and Phase-Splitting Forward Filter

By omitting the regressor filtering in (18) and/or (20), simplified versions of the algorithm described by (23) - (28) can be derived. The partial derivation of $|y(n)|^2$ with respect to $\boldsymbol{w}_d$ is then approximated by Feintuch updates [8]-[10]. Applied to (18), the second term in (19) vanishes and (27) simply becomes $\zeta_i^{(l)}(n) = r(n-i)$, so that the prefilter of state $\boldsymbol{X}_R^{(l)}(n)$ can be omitted. Applied to the gradient of the feedback filter, (21) becomes $\psi_i^{(l)}(n) = y(n-i)$, so that vector $\boldsymbol{X}_A(n)$ in (28) is approximated by $\boldsymbol{X}(n)$ and the lattice prefilter with state $\boldsymbol{X}_A(n)$ becomes redundant.

If the introduced algorithm is employed to passband equalization, the feedforward filter can be considered as a Hilbert transformer generating the analytic (complex-valued) signal, followed by two real-valued equalizers which are theoretically identical. These two tasks are combined into one filtering operation. The forward filter has therefore to be initialized as a phase splitter, which can be chosen as the pulse-shaping transmit filter employed at the transmitter. This is in contrast to equalization in baseband domain, for which phase-splitting is performed by a mixer and the forward equalizer can be initialized by a single spike.

We apply the phase-splitting equalizer introduced in [11] for passband equalization, which implements the feedforward filter as two real-valued filters and omits the cross-coupling between these filters. The resulting hardware efficient equalizer requires half as many real-valued multiplications per symbol as the complex-valued filter.

D. Switching to Tracking Mode

When converged, the equalizer is switched to a DFE, updated by standard least mean squares (LMS) algorithm. CM receivers are generally supposed to be located in the vicinity of the corresponding DFE [8]. We can however further minimize the probability of getting trapped in a local minimum of the DFE cost function by applying a soft decision device introduced in [12] for the sake of higher MSE, as then the amplitude of the feedback filter's input signal reduces for low MSE, reducing the probability of error propagation.

The decision error applied for updating of the DFE's feedforward filter has to be backrotated by $e^{j\theta}$. As the (hard or soft) decision is a bounded signal, stability monitoring becomes redundant. The feedback filter can therefore be switched to a direct form implementation requiring the halved number of multiplications compared to a lattice implementation. This results either in power saving or allows increasing the number of filter taps (forward or feedback) with the same number of employed multipliers. The latter is advantageous, as equalizers adapted by stochastic gradient descent algorithms, like CMA, exhibits an excess mean square error due to adaptation noise which increases with increasing number of filter taps. For CMA operating on non-CM constellations, this noise gets relatively high. As the CMA-adapted start-up equalizer has only to succeed in opening the eye, while the symbol error rate during DD equalization should be much lower, it was suggested in [13] that the latter shall generally consist of more taps than the equalizer during acquisition.

A recursive algorithm for the calculation of $\boldsymbol{a}$ ($\boldsymbol{a}^{(M)}$ in (29)) from $\boldsymbol{k}$ can be derived from (16). It is given by

$$\boldsymbol{a}^{(1)} = k_1, \qquad \boldsymbol{a}^{(m)} = \begin{bmatrix} a_1^{(m-1)} + a_{m-1}^{(m-1)} k_m \\ a_2^{(m-1)} + a_{m-2}^{(m-1)} k_m \\ \vdots \\ a_{m-1}^{(m-1)} + a_1^{(m-1)} k_m \\ k_m \end{bmatrix}^T . \tag{29}$$

This calculation can be performed offline, assuming the channel to be only slowly time-varying.

If the MSE in tracking mode raises over a predefined value, caused e.g. by a sudden change in the channel characteristics or an emerging strong disturber, the equalizer is switched back to acquisition mode. We suggest to set the parameters of $\boldsymbol{k}$ then to zero, as the feedback filter of a DFE is not generally minimum phase and therefore the corresponding IIR filter may be instable. The set of feedforward filter coefficients may however serve as a new starting coefficient set.

E. Determination of the Modulation Technique

Whether QAM or CAP transmission scheme is employed can easily be determined by

$$E\{|Y - \hat{A}'|\} - E\{|Y - \hat{A}|\} \begin{array}{l} < 0 \rightarrow \text{QAM sent} \\ > 0 \rightarrow \text{CAP sent} \end{array} . \tag{30}$$

The expectations in (30) can be approximated by averaging over a number of p symbols. A simple technique is therefore to switch the symbol rotator in Fig. 1 alternatingly on and off every p symbols and measure the resulting MSE. If it drops below a specified constellation-dependent threshold for switching to DD-mode while the rotator is active, the transmission scheme is detected as QAM, otherwise as CAP. This technique has no crucial influence on the phase error estimator, as during periods of incorrect constellation rotation the phase error can be viewed as a random signal. The misadjustment vanishes then therefore in the mean.

If QAM transmission has been determined from (30), the tap weights of the feedback filter have to be rotated before switching to the DFE structure, as the feedback filter of the DFE is fed by the sliced symbols, which have already been backrotated. Consider the direct form filter whose taps weights are calculated by means of (29). Its output is given by

$$y_k = u_k - \sum_{p=1}^{N} a_p y_{k-p} . \tag{31}$$

If its input signal is backrotated, (31) becomes

$$y_k e^{-j\omega_c T} = u_k e^{-j\omega_c T} - \sum_{p=1}^{N} \tilde{a}_p y_{k-p} e^{-j(p+1)\omega_c T} . \tag{32}$$

Equations (31) and (32) coincide, if the tap weights in (32) are rotated, i.e. the tap weights of the feedback filter in the starting period, denoted as a_{IIR} are rotated representatives of the weights required in the tracking period a_{DD} according to

$$a_{DD_k} = a_{IIR_k} e^{j\omega_c kT} . \tag{33}$$

This simple transformation can also be performed offline.

IV. Simulation results

We present simulation results for the dual-mode algorithm in a scenario similar to the one introduced in [1], with carrier frequency f_c set to 15 MHz and $1/T$ = 25.92 Mbaud. Either 16-CAP or 16-QAM transmission is employed. A ∅ 0.5 mm VDSL1-TP1 loop [2] of length 250m has been chosen. Square-root raised-cosine pulse shaping filters with 15% excess bandwidth are employed as transmit-filters. The magnitudes of the transmit filter and the loop transfer functions are shown in Fig. 3. White noise with $\sigma_n^2 = 2 \cdot 10^{-5}$ is added to the receiver input signal. At the receiver side we employ a $T/3$ FS phase splitting forward equalizer with 48 taps, separately processing the in-phase and quadrature components of the input signal, which is initialized with the coefficient weights of the pulse-shaping transmit filters. The feedback filter consists of 10 taps. The number of taps remains unchanged during the simulations. The step-sizes of the two adaptive filters are set to 0.002 and 0.001 during starting and tracking period, respectively. They must not be chosen too high during acquisition, as

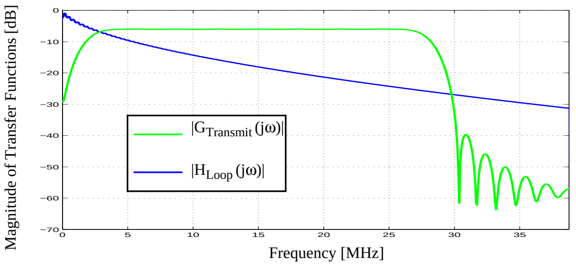

Fig. 3. Magnitudes of loop and transmit filter transfer functions for the considered scenario.

this violates the slow convergence property and the equalizer may then converge to wrong solutions, with output symbols located on a circle. The switch to DD-mode occurs, if the MSE calculated by the receiver drops below -16.7 dB.

In the first simulation the original algorithm is compared with the simplifications derived by the Feintuch approach. The resulting MSE curves (averaged over 100 symbols) for QAM transmission are shown in Fig. 4. The simplified algorithms show almost no performance degradation for the considered scenario.

The second simulation shows the algorithm's ability to blindly determine the transmission scheme. Resulting MSE curves for both schemes are shown in Fig. 5, each simulated with known and unknown transmission scheme. As expected, the resulting MSE gets very high during periods with wrong symbol rotation, the speed of convergence however does not suffer from the on and off turning of the symbol rotator. The true transmission scheme is identified in all cases.

V. Conclusion

In this paper, we presented a blind start-up technique for DFEs based on the IIR-CMA. For stability reasons, the feedback filter is implemented in two-multiplier lattice form, which allows easy stability monitoring. The algorithm is well suited for equalization in the passband domain, as the feedback filter is placed behind the forward filter in acquisition mode. The required phase-splitting is therefore implicitly performed by the forward filter and the feedback filter is fed with a complex signal. We further introduced an approach for blind determination whether QAM or CAP transmission is applied.

In tracking mode the structure is switched to the DFE with feedback filter implemented in direct form. The coefficients of its corresponding starting mode equalizer have therefore to be transformed by means of a simple recursive algorithm. If the transmission scheme is detected as QAM, the tap weights have furthermore to be rotated. In order to minimize the probability of getting trapped in a local minimum of the DFE cost function, the feedback filter is the favorably fed by soft decisions. Simplifications of the proposed algorithm, deduced by approximating the gradient signals by Feintuch updates, are also shown in this paper. Simulation results indicate only slightly performance degradation of the simplified algorithms.

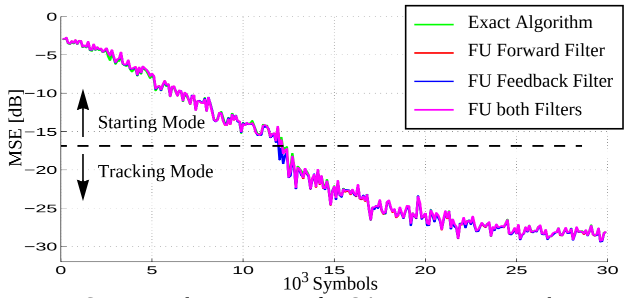

Fig. 4. MSE curves during start-up for QAM-transmission with exact algorithm and simplifications employing Feintuch updates (FU).

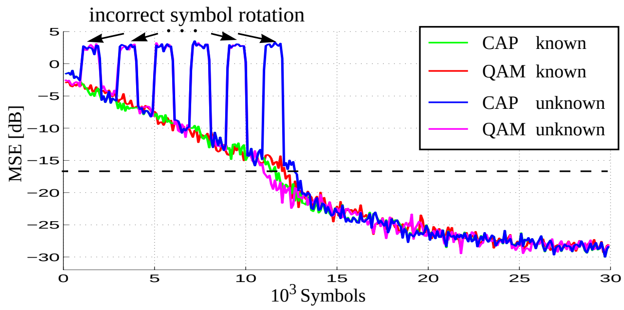

Fig. 5. MSE curves during start-up for QAM and CAP transmission with known and unknown transmission scheme.

References

[1] L.M. Garth, J. Yang, and J.J. Werner, "Blind equalization algorithms for dual-mode CAP-QAM reception," *IEEE Trans. Comm.*, vol. 49, no. 3, pp. 455-466, Mar. 2001.

[2] T1E1.4, "VDSL metallic interface - Part1: Functional requirements and-common specification," Draft Trial-Use Standard, Feb. 2001.

[3] J. Labat, O. Macchi, and C. Laot, "Adaptive decision feedback equalization: Can you skip the training period?," *IEEE Trans. Comm.*, vol. 46, no. 7, pp. 921-930, July 1998.

[4] D.N. Godard, "Self-recovering equalization and carrier tracking in two-dimensional data communication systems," *IEEE Trans. Comm.*, vol. 28, no. 11, pp. 1885-1911, Nov. 1980.

[5] P.A. Regalia, "On the convergent points of blind adaptive IIR equalizers," In *Proc. IEEE/EURASIP Workshop on Nonlinear Signal and Image Processing*, Baltimore, MD, June 3-6, 2001.

[6] K.X. Miao, H. Fan, and M. Doroslovacki, "Cascade lattice IIR adaptive filters," *IEEE Trans. Sig. Proc.*, vol. 42, no. 4, Apr. 1994, pp. 721-741.

[7] A. Bouttier, "A truly recursive blind equalization algorithm," In *Proc. IEEE Int. Conf. on Acoustics, Speech, and Sig. Proc.*, New York, May 1998, vol. 6, pp. 3381-3384.

[8] R.A. Casas, C.R. Johnson Jr., J. Harp, and S. Caffee, "On initialization strategies for blind adaptive DFEs," In *Proc. IEEE Wireless Comm. and Networking Conf.*, New Orleans, 1999, pp. 792-796.

[9] P.L. Feintuch, "An adaptive recursive LMS filter," *IEEE Proc.*, vol. 64, no. 11, pp. 1622-1624, Nov. 1976.

[10] C.R. Johson and M.G. Larimore, "Comments on 'An adaptive recursive LMS filter'," *IEEE Proc.*, vol. 65, no. 9, Sept. 1977, pp. 1402-1404.

[11] K.H. Mueller and J.J. Werner, "A hardware efficient passband equalizer structure for data transmission," *IEEE Trans. Comm.*, vol. 30, no.3, pp. 538-541, Mar. 1982.

[12] S.L. Ariyavisitakul and Ye Li "Joint coding and decision feedback equalization for broadband wireless channels," *IEEE Journal on Sel. Areas in Comm.*, vol. 16, no. 9, pp. 1670-1678, Dec. 1998.

[13] C.R. Johnson et al., "The Core of FSE-CMA behavior theory," *Unsupervised Adaptive Filtering*, Simon Haykin, ed., Wiley, New York, 1999.